Access to second stability region for coupled peeling-ballooning modes in tokamaks

H. R. Wilson and R. L. Miller

Citation: Phys. Plasmas 6, 873 (1999); doi: 10.1063/1.873326
View online: http://dx.doi.org/10.1063/1.873326
View Table of Contents: http://pop.aip.org/resource/1/PHPAEN/v6/i3
Published by the American Institute of Physics.

Access to second stability region for coupled peeling-ballooning modes in tokamaks

H. R. Wilson
ERATOM/UKAEA Fusion Association, Culham Science Centre, Abingdon Oxon, OX14 3DB, United Kingdom

R. L. Miller[a]
General Atomics, P.O. Box 85608, San Diego, California 92186-5608

(Received 1 September 1998; accepted 14 October 1998)

The peeling mode restricts access to the second stability region of the ideal ballooning mode at the tokamak plasma edge. Using a two-dimensional, high toroidal mode number eigenmode code employing a model tokamak equilibrium, it is shown that a window to second stability exists for a sufficiently deep magnetic well. The different mode structures of the various eigenmode branches are studied. In particular, when access to second ballooning stability exists, a ballooning mode perturbation at the first stability boundary can extend deep into the plasma core, and then instability is likely to result in large scale loss of plasma energy. © *1999 American Institute of Physics.* [S1070-664X(99)02703-2]

I. INTRODUCTION

The high confinement, ''H''-mode of tokamak operation makes it an attractive scenario for Next Step devices. The edge transport barrier, responsible for the high confinement, supports a steep pressure gradient which is widely believed to be limited by high toroidal mode number n ballooning modes. At a still higher pressure gradient, standard ballooning theory predicts the presence of a ''second stable'' region, and calculations show that it is possible to gain access to this second stable region if the magnetic shear is low. Increasing the depth of the magnetic well allows access with larger values of magnetic shear. This provides an opportunity for steeper edge pressure gradients in tokamaks, with a resulting improvement in performance, as observed in the good confinement H- or VH-modes (very high) of operation on DIII-D[1,2] and the Joint European Torus (JET),[3] for example.

To fully exploit second stability requires an understanding of edge magnetohydrodynamic (MHD) instabilities and their interaction. Huysmans[4] combined the stability diagrams for high n ballooning and low n kink modes to illustrate that the kink mode can restrict access to second stability, it being unstable for high current density close to the plasma edge (i.e., low magnetic shear there). In addition, the peeling mode,[5,6] which can be considered as the high n analog of the kink mode, can be destabilized when an edge current density flows and this can prevent access to second stability for equilibria with weak magnetic wells.[7] In this paper we include the peeling mode in our ballooning mode analysis to demonstrate that second stability access is possible at the plasma edge, though it requires a deeper magnetic well because of the interaction between the peeling and ballooning modes than consideration of the individual modes would suggest. In addition, we calculate the radial structure of the marginally stable modes, showing that this can be quite different in different regions of parameter space; this is illustrated by both edge localized structures and structures which extend deep into the plasma interior.

We present the essential features of the stability diagram and mode structure by restricting consideration to a simple tokamak equilibrium model, analogous to the so-called $s-\alpha$ model,[8] which is known to reproduce many of the qualitative features of ballooning modes calculated from true tokamak equilibria. While this model contains sufficient physics to demonstrate the important qualitative properties of coupled peeling–ballooning modes, it cannot replace the analysis of a full tokamak equilibrium, and the development of a stability code to address this is under way. This study of the $s-\alpha$ model therefore serves as a first indication of the properties of coupled peeling–ballooning modes, and also as a guide to the features which a general geometry code must capture.

The $s-\alpha$ model is based upon a large aspect ratio expansion of a finite β (β is the ratio of plasma pressure to magnetic field pressure), circular cross-section toroidal plasma. The pressure gradient is assumed to be locally large in the vicinity of the rational surface close to the plasma edge, about which we expand. This expansion of the equilibrium is valid provided the mode is radially localized. Thus, the equilibrium can be characterized by six parameters: the magnetic shear, $s=rq'/q$; the pressure gradient parameter $\alpha=-2\mu_0 Rq^2p'/B^2$; the distance of the first vacuum rational surface from the plasma surface in units of the distance between rational surfaces, Δ; the magnetic well proportional to d_M (such that the Mercier coefficient $D_M=\alpha d_M/s^2$ [9]), and the edge safety factor q (here r is the minor radius, a prime denotes a derivative with respect to r, R is the major radius, p is the plasma pressure and B is the magnetic field). A linear radial variation of α, proportional to the parameter α_d, provides a means to determine the radial mode structure of ballooning modes, and the magnetic shear is taken to be constant for simplicity. The toroidal mode number n is assumed to be large.

[a]Present address: Archimedes Technology Group, San Diego, California 92186.

II. NUMERICAL RESULTS

Following a minimization of the change in energy associated with a small plasma displacement, a set of coupled equations for the Fourier harmonics of the radial component of the displacement, $u_m(x)$ has been derived,[7] which can be solved to determine their dependence on the radial coordinate $x=m_0-nq$:

$$s^2(x-M)^2\frac{d^2u_m}{dx^2}+2\,s^2(x-M)\,\frac{du_m}{dx}-(x-M)^2u_m-\alpha\left\{s\left[(x-M)^2+\frac{1}{2}\right]\frac{d}{dx}[u_{m+1}-u_{m-1}]+s(x-M)\,\frac{d}{dx}[u_{m+1}+u_{m-1}]\right.$$
$$\left.+s(x-M)\,[u_{m+1}-u_{m-1}]-\frac{1}{2}[u_{m+1}+u_{m-1}]-d_Mu_m\right\}-\frac{\alpha^2}{2}\left\{[(x-M)^2+1]\right.$$
$$\left.\times\left(u_m-\frac{1}{2}[u_{m+2}+u_{m-2}]\right)-(x-M)[u_{m+2}-u_{m-2}]\right\}=0. \tag{1}$$

Here $m=m_0$ is the poloidal mode number associated with the first rational surface outside the plasma, assumed large, so that $x=\Delta$ represents the plasma surface and x increases going into the plasma; the shifted poloidal mode number $M=m_0-m$ also increases into the plasma (i.e., $x=M$ are the locations of the rational surfaces). Terms of order $1/n$ have been neglected. To represent equilibrium radial profiles (important to deduce the radial structure of ballooning modes) we express

$$\alpha=\alpha_a-\frac{\alpha_d}{nq_as}(x-\Delta), \tag{2}$$

where the subscript a represents the edge value of the parameter. Boundary conditions at the plasma–vacuum interface are obtained by matching to the vacuum solution for magnetic field fluctuations (for which a cylindrical model is adopted); thus, at $x=\Delta$ we impose

$$(\Delta-M)\left\{-s(\Delta-M)\,\frac{du_m}{dx}-[2-(\Delta-M)]\,u_m\right.$$
$$\left.+\frac{\alpha}{2}(\Delta-M)\,(u_{m+1}-u_{m-1})\right\}_{x=\Delta}=\Omega^2u_m, \tag{3}$$

where Ω^2 is an eigenvalue such that $\Omega^2<0$ corresponds to instability (we are interested in marginal stability, for which $\Omega^2=0$). Deep in the core, in the limit $x\to\infty$, the condition $u_m(x)=0$ is applied.

Two different types of mode can be deduced from Eqs. (1) and (3). First, employing the local expansion, valid for modes localized around a single vacuum rational surface close to the plasma–vacuum interface, i.e., $\Delta\ll1$, the peeling mode criterion is found:

$$\alpha>\frac{2\,(2-s)}{-\,d_M}, \tag{4}$$

for stability. Second, employing the ''ballooning approximation'' for radially extended modes, $u_m(x)\simeq e^{imk}u(x-m)$, we derive the familiar $s-\alpha$ equation from Eq. (1):

$$\frac{d}{d\eta}\left\{[1+h^2(\eta)]\,\frac{dy}{d\eta}\right\}+\lambda\,\alpha\Gamma y=0, \tag{5}$$

where η is the ballooning angle, $h(\eta)=s(\eta-k)-\alpha\sin\eta$ and $\Gamma=\cos\eta+h\sin\eta+d_M$. An ''intermediate'' eigenvalue λ has been introduced, with the physical situation $\lambda=1$ corresponding to marginal stability contours in the $s-\alpha$ plane for a given magnetic well d_M. The boundary conditions on Eq. (5) are that y, which is the Fourier transform of u, tends to zero at large $|\eta|$, and we choose k to maximize the unstable region.

If the coupling between peeling and ballooning modes is neglected, then for a deep magnetic well $d_M=-0.6$, typical of advanced tokamak scenarios, one obtains the stability diagram shown in Fig. 1(a) from Eqs. (4) and (5); thus, there appears to be access to the second stability region. However, if we calculate the stability diagram by solving the more complete Eqs. (1) and (3), then we observe a strong coupling between the peeling and ballooning modes and there is no

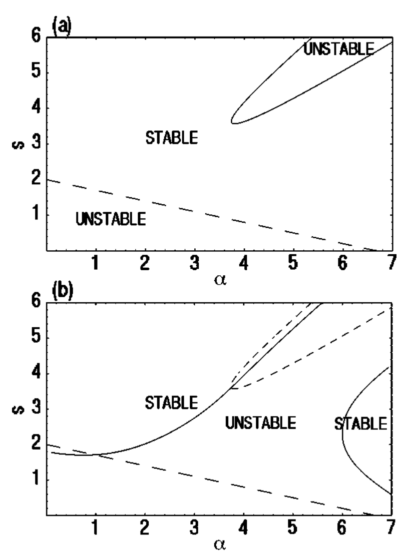

FIG. 1. The marginal stability contours in the $s-\alpha$ plane for a magnetic well parameter $d_M=-0.6$ for (a) the ideal $n=\infty$ ballooning (full) and localized peeling (dashed) modes and (b) the marginal stability contours from the two-dimensional edge MHD code for the same magnetic well and $\Delta=0.1$, $q=4$, $n=20$, $\alpha_d=4.0$ (full curve) compared to the ideal ballooning (short-dashed) and peeling (long-dashed) boundaries.

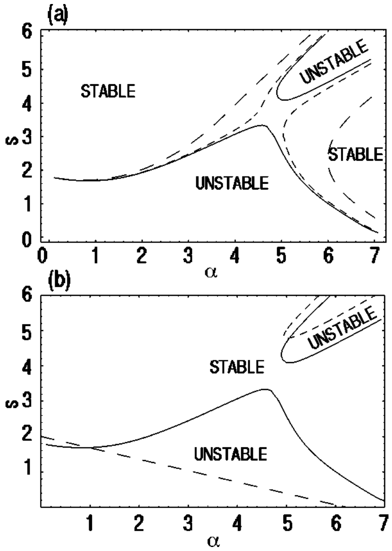

FIG. 2. (a) A sequence of marginal stability curves from the two-dimensional stability calculation as the magnetic well is deepened from $d_M = -0.6$ (long-dashed), through $d_M = -0.64$ (short-dashed), to $d_M = -0.645$ (full), showing access to second stability at the deepest well (the other parameters as Fig. 1). In (b) the results of the two-dimensional code (full curves) are compared with the individual peeling and ballooning stability boundaries for $d_M = -0.645$.

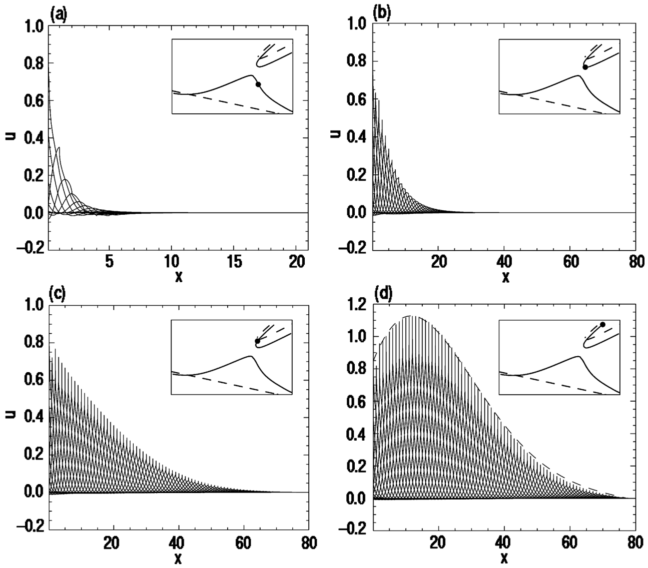

FIG. 4. The radial eigenmode structures for the Fourier components $u_m(x)$ for (a) the peeling mode branch at $\alpha = 5.0$, $s = 2.58$; (b) the second stable branch at $\alpha = 5.0$, $s = 4.09$; (c) close to the "nose" of the $n = \infty$ ballooning mode marginal stability contour at $\alpha = 5.0$, $s = 4.67$, and (d) on the first stable branch at $\alpha = 6.0$, $s = 6.13$; parameters are as for Fig. 2(b). In (d), the dashed curve shows the fit to the Airy function given in Eq. (6). The insets show the position in the $s - \alpha$ diagram.

access to second stability for this value of the magnetic well [Fig. 1(b)]; note, however, that a second stability region does exist. Here we have chosen $n = 20$ and a small value of $\Delta = 0.1$, for which the localized peeling mode stability criterion is expected to be accurate when coupling to the core Fourier harmonics is weak (i.e., low α).

As the well is deepened further, the unstable region gets smaller and, for $d_M \lesssim -0.64$, access to second stability can be achieved. Figure 2 shows the effect of progressively deepening the magnetic well from $d_M = -0.6$ through $d_M = -0.64$ and finally to $d_M = -0.645$, with other parameters the same as Fig. 1. It is interesting to note that in the case $d_M = -0.645$ the marginal stability boundary is pulled above the peeling mode stability criterion as it passes under the nose of the ballooning boundary [Fig. 2(b)]. For larger $\Delta = 0.9$ the localized peeling mode stability criterion is no longer valid, and the stability curves predicted by the two-dimensional calculation are somewhat different to the low Δ case. These results are shown in Fig. 3 for $d_M = -0.6$ (no

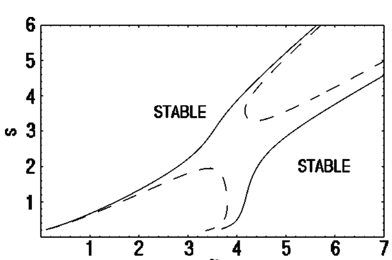

FIG. 3. The marginal stability contours calculated using the two-dimensional code for $\Delta = 0.9$ and $d_M = -0.6$ (full curve) and $d_M = -0.62$ (dashed curve); the other parameters are as for Fig. 1(b).

second stability access) and $d_M = -0.62$ (second stability access).

The structure of the modes is very different for different parts of the marginal stability curves: this can be illustrated by considering the $\Delta = 0.1$ case shown in Fig. 2(b). Taking $\alpha = 5.0$, $s = 2.58$, corresponding to marginal stability on the low shear peeling mode branch, we find that the mode is very localized at the plasma edge, coupling only a few internal rational surfaces, but several (seven in this case) vacuum surfaces [Fig. 4(a)]. If we now consider higher shear, $s = 4.09$, at the same value of α, so that we are on the second stability branch of the ballooning mode marginal stability contour, then we find the mode structure shown in Fig. 4(b). There are now many more Fourier modes that are resonant inside the plasma, which peak at their respective rational surfaces, as expected from a ballooning mode. Approximating the fraction of plasma minor radius which this mode penetrates the plasma by $\delta r / r \sim \delta m / (nqs)$, where δm is the number of internal Fourier modes, we find $\delta r / r \sim 6\%$, which justifies the "localized mode" approximation we made in performing the equilibrium expansion. We find that this mode structure persists as we reduce α towards the first stability branch, up to the point at which this branch crosses the $n = \infty$ ideal ballooning stability contour. Then the mode structure becomes much more radially extended, as shown in Fig. 4(c), which is for a case just below the $n = \infty$ ballooning mode boundary, again at $\alpha = 5.0$, but $s = 4.67$. Finally, as we increase α and s along the first stability boundary, the ballooning nature begins to dominate and the mode amplitude peaks away from the plasma edge; this is illustrated for the case $\alpha = 6.0$, $s = 6.13$ in Fig. 4(d). This mode structure is similar to those derived previously,[7] where the envelope of the $u_m(x)$ was shown to be an Airy function.[10] If we fit a shifted Airy function of the form

$$C(x)=a\{\mathrm{Ai}[c\,(x-d)]+b\,\mathrm{Bi}[c\,(x-d)]\}, \tag{6}$$

then we obtain good agreement for $a=2.104$, $b=-\ 0.014$, $c=0.056$, $d=29.86$ as shown by the dashed curve in Fig. 4(d). The small amount of Bi which is included is to take account of the finite value of the maximum x range; a is an arbitrary normalization; the shift d is adjusted to match the position of the maximum in the envelope, and the width of the eigenfunction is matched through the parameter c. If we take the edge ballooning theory derived in Ref. 7, then this provides a prediction for c:

$$c=\left(\frac{2\,\lambda_\alpha \alpha_d}{\lambda_{kk}\,nqs}\right)^{1/3}, \tag{7}$$

where $\lambda_\alpha \equiv \partial\lambda/\partial\alpha$ and $\lambda_{kk}\equiv\partial^2\lambda/\partial k^2$. Solving the ballooning equation (5) around the marginal stability point $\alpha=6.0$, $s=6.13$ we find that $\lambda_\alpha=-0.19$, $\lambda_{kk}=26.8$, so that $c=0.049$. While this is close to the fitted value, the deviation is significant (due to the 1/3 exponent), and indicates that the high n expansion procedure is beginning to break down due to the high value of λ_{kk} calculated here (comparable to n).

III. CONCLUSION

We have demonstrated that access to a second stable region to coupled peeling–ballooning modes is possible at the edge of a tokamak plasma, provided the magnetic well is sufficiently deep. The stable region in the $s-\alpha$ diagram is reduced due to the coupling between the two modes, which also makes access to the second stable region more difficult. When access to second stability exists, there are three distinct mode structures which can be identified: a peeling mode structure at low magnetic shear, which is very localized at the edge, a structure on the second marginal stability branch which has relatively more Fourier modes, penetrates deeper into the plasma, and has a ballooning nature, and a structure on the first marginal stability branch which has many Fourier modes and is very radially extended, penetrating deep into the plasma. An important conclusion we draw is that if access to second stability exists at the plasma edge, then the consequences of entering the ballooning unstable region are likely to be dramatic: the resulting instability is expected to increase transport to reduce α, further enhancing the instability and leading to a crash event as the plasma equilibrium adjusts towards the first stability boundary. Furthermore, because these modes extend deep into the plasma core they would presumably result in turbulent heat loss over a large radial region, which could be catastrophic for confinement. It is therefore important to confirm these stability and mode structure features in a more realistic geometry, and work is under way to develop the numerical tools required for such a study.

ACKNOWLEDGMENTS

H. R. W. would like to thank General Atomics for their hospitality during his visit.

This work was funded jointly by the U.K. Department of Trade and Industry and Euratom, and by the U.S. Department of Energy under Grant No. DE-FG03-95ER54309. This work was made possible in part by the EU–US Bilateral Agreement.

[1] T. H. Osborne, R. J. Groebner, L. L. Lao, A. W. Leonard, R. Maingi, R. L. Miller, G. D. Porter, D. M. Thomas, and R. E. Waltz, in *Proceedings of the 24th European Physical Society Conference on Controlled Fusion and Plasma Physics*, Berchtesgaden, 1997 (European Physical Society, Petit-Lancy, Switzerland, 1997), Part III, p. 289.

[2] G. L. Jackson, J. Winter, T. S. Taylor *et al.*, Phys. Fluids B **4**, 2181 (1992).

[3] N. Deliyanakis, D. P. O'Brien, B. Balet, C. M. Greenfield, L. Porte, A. C. C. Sipps, P. M. Stubberfield, and H. Wilson, Plasma Phys. Controlled Fusion **36**, 1159 (1994).

[4] G. T. A. Huysmans, C. D. Challis, M. Erba, W. Kerner, and V. V. Parail, in *Proceedings of the 22nd European Physical Society Conference on Controlled Fusion and Plasma Physics*, Bournemouth, 1995 (European Physical Society, Geneva, 1995), Part I, p. 201.

[5] D. Lortz, Nucl. Fusion **15**, 49 (1975).

[6] J. A. Wesson, Nucl. Fusion **18**, 97 (1978).

[7] J. W. Connor, R. J. Hastie, H. R. Wilson, and R. L. Miller, Phys. Plasmas **5**, 2687 (1998).

[8] J. W. Connor, R. J. Hastie, and J. B. Taylor, Phys. Rev. Lett. **40**, 396 (1978).

[9] C. Mercier, Nucl. Fusion **1**, 47 (1960); and Nucl. Fusion Suppl. **2**, 801 (1962).

[10] *Handbook of Mathematical Functions*, edited by M. Abramowitz and L. A. Stegun (Dover, New York, 1965), p. 441.